

Kinetic and Isotherm Studies of Al (III) Ions Removal from Aqueous Solution by Adsorption onto Coula edulis Nut Shell Activated Carbon

Mexent ZUE MVE^{1*} Raphinos KOUYA BIBOUTOU¹ François EBA¹ David NJOPWOU²
1.Laboratoire Pluridisciplinaire des Sciences (LAPLUS) de l'École Normale Supérieure (ENS-GABON)
BP 17009 Libreville – Gabon
2.Laboratoire de Physico-chimie des Matériaux Minéraux, Université de Yaoundé I,
B.P 812 Yaoundé (Cameroun)

Abstract

The adsorption of Al (III) ions onto coula edulis activated carbon was performed at using batch protocol. The experiments were accomplished as function of several parameters such as: pH (2-4), initial concentration (159.1-1006.6 mg/L), contact time (10-120 min.), and temperature (25-60 °C). The adsorption capacity of Al (III) ions increased when pH, initial concentration and / or contact time increased and decreased when temperature increased. The adsorption data was fitted by Langmuir isotherm model rather than Freundlich isotherm model. Kinetic study revealed an adsorption process following the pseudo-second order model. Thermodynamic parameters gave negative value of enthalpy change, which corresponded to an exothermic process and negative value of entropy change which indicated a more ordered distribution of Al (III) ions in solid phase rather than in liquid phase. The free energy change was found positive in all the studied temperatures range. The effectiveness of the reaction is supported by supplementary energy produced by agitation.

1.Introduction

The presence of certain metallic ions in water is a worrying environmental problem due to their toxicity, poor biodegradability and high persistence in the environment (**Wan et al., 2008**). Among these metallic species, aluminium is that which is the most abundant in air, soil and water. Consequently, human exposure to aluminium is potentially possible, because of its large dissimulation in the human environment. Aluminium is used: (i) as ingredient or excipient in pharmaceuticals and industrial foods; (ii) as flocculating agent in potable water treatment. (iii) The use of aluminium as metal for the making of kitchen cookers and food packaging. Despite the establishment of a clear correlation between a manifestation of a sickness and exposure to aluminium, many diseases seemed be caused by inhalation or ingestion of high level of aluminium. That is the cause of Alzheimer's disease, renal insufficiency, encephalopathy, pulmonary fibrosis, microcytic anaemia and disturbances of the sleeping (**Miu et al., 2006**). It is then important that the level of aluminium in public water supplies be low. In some countries and international organization such as Canada and World Health Organisation (WHO), the Al (III) species concentrations does not exceed 0.1 mg/L and 0.2 mg/L respectively in potable water (**Takassi et al., 2015**).

Many methods have been used in the removal of metallic ions from wastewaters. That is the case of precipitation, electro deposition, ultrafiltration, exchange membrane (**Pranay et al., 2015**). Adsorption, a physicochemical method was chosen in this work because of its efficiency in waste water treatment process, which is gaining prominence as means of producing high quality effluents, which contain low level of metal ions.

The high cost of activated carbon used as adsorbent in adsorption process leads to the research of adsorbents with low-cost from industrial and agricultural wastes. A limited report of those materials includes: teanut hull-based (**Zhuo-Ya et al., 2012**), tea waste (**Isil et al., 2012**), Gigartina Acicularis Biomass (**Hassouni et al., 2013**), Bamboo (**Qing-Song et al., 2010**), palm nut shells (**Bamba et al., 2009**) and coconut shells (**Veena et al., 2012**).

The objective of this study concerns the valorisation of Coula edulis nut shell, a waste biomass collected at the markets of Libreville (Gabon) at preparing activated carbons and determining their capacity as adsorbents through of the removal of Al (III) ions from the aqueous solutions.

2.Materials and Methods

2.1. Preparation of activated carbons: Coula edulis nut shells were collected at Libreville markets and were washed with distilled water to remove the surface adhered particles, then dried in oven at 110°C for 24 h. They were heated at 600°C during 5 hours and cooled to ordinary temperature. They were then milled and sieved to obtain particles sized in diameter range of 0.83 to 1 mm. The powder of activated carbon was then washed with demineralized water, filtered and dried in an oven at 110°C for 24 hours. A fraction of activated carbon is plunged into a solution of HCl (HAC) or in a Zn²⁺ salt (ZAC) solution during 48 hours at 120°C, washed with demineralized water under the obtainment of a pH in the order of 6.5. This constituted a chemical activation,

while a simple pyrolyzed of fraction coula edulis nut shell was considered as physically activated carbon (ACo). The final powder is preserved in a tight glass for use as adsorbents.

2.2. Characterization of Coula edulis activated carbons

The characterization of Coula edulis activated carbons as presented in a previous study (Zue Mve et al., 2016) concerns: (i) the Boehm determination of their acid-basic properties; (ii) the potentiometric determination of point of zero charge (pHpzc); (iii) the determination of the specific surface according iodometric method; (iv) the analysis of the inorganic chemical composition and (v) the determination of the main groups by the FTIR analysis.

2.3. Batch Adsorption Studies

Batch experiments were conducted to study the factors affecting the adsorption of Al (III) onto ACo, HAC and ZAC. In a flask of 25 mL was added at the beginning of each experimental run, a known weight of activated carbon (0.2 g) was added to 25 mL solution containing a known concentration of aluminium (III) ions. The studied factors were pH (2 - 4), initial ion concentration (159.1; 244.5; 413.6; 824.39 and 10006.6 mg/L), contact time (30- 240 min) and temperature (298 to 333 K). The flasks were agitated in a shaking water bath at 200 rpm constant rate until the equilibration time of the interaction was reached. The mixture was then filtered and the remaining aluminium concentrations were determined by ICP-AES.

The amount of ions adsorbed per unit mass, q_e (mg/g), was calculated by the following equation:

$$q_e \left(\frac{\text{mg}}{\text{g}} \right) = \frac{(C_0 - C_e) * V}{m} \quad [1]$$

Where C_i and C_e are the ions concentrations at the initial time and at given time of interaction (mg/L), respectively; V is the volume of the solution (L) and m the mass of adsorbent used (g).

3. Results and Discussions

3.1. Characterization of Coula edulis activated carbon

Many properties of Coula edulis activated carbons have been previously studied (Zue Mve et al., 2016). Results related to the acid-basic properties, the determination of the pH of point of zero charge, iodine number and specific surface, the inorganic chemical composition analysis and FT-IR characteristics of coula edulis activated carbon are shown in Table 1, 2, 3 and 4 respectively.

3.2. Effect of initial pH

The variation of Al (III) ions uptake as a function of pH by activated carbon is described by the plots shown in Figure 1.

It was showed that the removal of Al^{3+} ions uptake increased as the pH of the suspension increased. The lowest aluminum ions adsorbed were obtained at pH 2, what may be caused by the competitive effect between H^+ ions Al (III) ions for the access at the available adsorbent sites. At $\text{pH} > 2$, the concentration of H^+ decreased gradually, the interaction adsorbent-adsorbate concerns preponderantly Al (III) ions and adsorption sites on the surface of activated carbon. That permitted the access on the available adsorption sites onto the activated carbon surface to a gradually great number of Al (III) ions. The amount of Al (III) ions adsorbed per unit mass is then progressively growing. Similar results have been reported by Hayat *et al.*, (2013).

3.3. Effect of initial concentration

The effect of initial concentration (Figure 2) of Al (III) was studied at varying the initial concentration of Al (III) from 159.1 to 1006.6 mg/L.

The results reported in Figure 2 illustrated the dependence of the amount of Al (III) ions adsorbed against the initial concentration in Al (III) ions. It is observed the increase of the Al (III) ions uptake with the increase in the initial concentration of Al (III) ions solutions. A comparative behavior is reported by (Takassi *et al.*, 2015). It could be explained if it is considered the fact that, the number of available adsorbent sites is higher to that of solute species. Then, the increase in concentration of Al (III) solutions causes the increase of solute species that leads to a progressive increase of amount of Al (III) ions adsorbed under the obtainment of saturation of adsorbent sites.

3.3.1. Applicability of adsorption isotherm models

The experimental data on the isotherm adsorption have been subjected to the applicability of the Langmuir (Langmuir, 1918) and Freundlich (Freundlich, 1906) isotherm models.

The Langmuir isotherm and Freundlich isotherm models in their linear forms are expressed respectively by the equations:

$$\frac{C_e}{q_e} = \frac{1}{q_m K_L} + \frac{C_e}{q_m} \quad [2]$$

And

$$\ln q_e = \ln K_f + \frac{1}{n} \ln C_e \quad [3]$$

Where, K_L (L/mg) and q_m (mg/g) are Langmuir isotherm constants related to respectively. And K_F (mg/g) and n are Freundlich isotherm constants related to respectively.

Langmuir equilibrium or separation factor (R_L), which characterizes the adsorption, is defined by the following equation:

$$R_L = \frac{1}{(1+K_L C_0)} \quad [4]$$

Where, C_0 is the initial concentration of the Al (III) ions solutions (mg/L). The R_L value indicates the mode of sorption of the isotherm process, if the process is unfavourable ($R_L > 1$) or linear ($R_L = 1$) or favourable ($0 < R_L < 1$) or irreversible ($R_L = 0$). Plotting of C_e/q_e versus (C_e) results straight line as shown in Fig. 3 of slope $1/q_m$ and intercept $1/K_L q_m$. And the plots of $\ln(q_e)$ versus $\ln(C_e)$ give straight line of slope $1/n$ and intercept $\ln(K_f)$ as presented in Fig. 4.

The Langmuir and Freundlich constants for the adsorption isotherm models and statisticals are summarized in Table 5.

The Langmuir energetic constant K_L and the maximum monolayer adsorption capacity q_m varied in the identical manner: K_L and q_m for ZAC have been found higher to those of ACo and HAC with correlation coefficient in the order of the unity. The Langmuir separation factor R_L showed values in the order of 1, which corresponded to a favorable adsorption process.

The Freundlich maximum multilayer capacity K_f (mg/g) and intensity factor n of ZAC were found classified as: ZAC > ACo > HAC. The intensity factor was found higher to unity which corresponded to a favorable adsorption.

3.4. Kinetic studies

3.4.1. Effect of contact time

The effect of contact time on the of Al (III) ions uptake was carried out at varying the duration of interaction Al (III) ions-activated carbon from 10 to 120 minutes of a suspension of 0.2 g of activated carbon into 25 mL of Al (III) ions solution (Figure 5).

The curves of the variation of adsorption capacity of Al (III) ions as a function of time presented the same shape on each of the activated carbons. It was observed a significant increase in the adsorption capacity of Al (III) ions from 10 minutes to about 40 minutes before equilibrium sets. In the first step, the elimination of Al (III) ions was mainly due to the transfer of Al (III) ions from solution to the surface of the adsorbents. And the last step go from 40 to 120 minutes was characterized by saturation of adsorption sites or by the intra particle transport in the pores of activated carbons. This behavior during adsorption of metal ions is the same as that observed by Ketcha et al., (2015) during the adsorption of Mn (II) ions onto the granules and modified activated carbons. The saturation time is nearly the same for all activated carbons indicating that these activated carbons have similar porosity.

3.4.2. Adsorption kinetic studies

The experimental variations of the adsorption capacities as a function of time were carried out using pseudo-first order and/or pseudo-second order kinetic models (Lagergren, 1898; Ho and McKay, 2002).

The Lagergren first order equation (5) is represented by the equation (5):

$$\ln(q_e - q_t) = \ln q_{e1} - \frac{K_1 t}{2.303} \quad [5]$$

Where q_e and q_t are the amounts of Al (III) adsorbed (mg/g) at equilibrium and at time t , respectively and K_1 is the rate constant of first order kinetic adsorption (min^{-1}). Pseudo-first order parameters, q_e (cal) and K_1 , at different concentrations are calculated from the slope and intercept of the linear plots of $\ln(q_e - q_t)$ versus t (Figure 6).

The pseudo second order rate equation (6) is represented by the equation (6)

$$\frac{t}{q_t} = \frac{1}{K_2 q_e^2} + \frac{t}{q_{e2}} \quad [6]$$

Where K_2 is the rate constant of second order kinetic adsorption (g/mg.min). Pseudo second order parameters, q_e (cal) and K_2 , are calculated from the slope and intercept of linear plots t/q_t versus t as shown in Fig. 7.

It appears in this study, that the representative curves of the pseudo-first order equation were found straight, with correlation coefficients of less than 0.95. The kinetic constants values (K_1) of 0.023, 0.269 and 0.0233 min^{-1} for ACo, HAC and ZAC respectively. In addition, the deviation percentages were 42.24%, 59.19% and 64.75% respectively. These last results showed the high difference between the theoretical adsorption capacities and the experimental adsorption capacities and confirmed that the adsorption kinetics of Al (III) ions

to the ACo, HAC and ZAC did not follow the first order.

The kinetic constants of the pseudo second order model (K_2) were 3.59×10^{-3} , 6.77×10^{-3} and $9.41 \times 10^{-3} \text{ min}^{-1}$ with correlation coefficients higher than 0.95. The values of the deviation percentages were less than 15% for all activated carbons. The latter observation shows that the theoretical adsorption capacities were comparable to those obtained experimentally. These results indicated that the adsorption of Al (III) ions adhered to the kinetics of the pseudo-second order. Similar results were found by Singh and Balomajumder et al., (2015).

3.4.3. Adsorption mechanism study

The adsorption mechanism was examined using: (i) (ii) liquid film diffusion model (Boyd et al., 1947) and intraparticle diffusion by Weber-Morris theory model (Weber and Morris, 1963). Their corresponding equations are given by the expressions respectively:

$$\text{Liquid film diffusion model is expressed as: } -\ln\left(1 - \frac{q_t}{q_e}\right) = K_{id2}t \quad [7]$$

$$\text{Intraparticle diffusion model expressed as: } q_t = K_{id1}t^{1/2} + C \quad [8]$$

Where K_{id1} and K_{id2} are respectively the intra-particle diffusion and liquid film diffusion rate constants. The parameters of each model have been calculated from the slopes and intercepts of linear plots q_t versus $t^{(1/2)}$ and

$-\ln(1 - q_t/q_e)$ versus t respectively (Figure 8 and 9 respectively). The results are reported in Table 8.

Figure 8 and 9 showed plots of the model used for the intraparticle and liquid film diffusion process onto activated carbons (ACo, HAC, and ZAC). The intraparticle diffusion constant, K_{id1} , K_{id2} and R^2 are given in Table 7.

If the intra-particle diffusion or the liquid film diffusion was the adsorption mechanism model, the plots might have zero intercept (varies from 4.3686 to 8.1219 for intra-particle diffusion model and from 0.5489 to 1.0428 with liquid film diffusion model) (Eba et al., 2010; Gupta et al. 2008). Despite, the plots being linear, the correlation coefficients (R^2) of intraparticle diffusion model 0.8084 (ACo), 0.7363 (HAC) and 0.6855 (ZAC) were lower compared to those of pseudo second order, 0.9916 (ACo), 0.9964 (HAC) and 0.9984 (ZAC). Correlation coefficients of liquid film diffusion 0.8758 (ACo), 0.7308 (HAC) and 0.821 (ZAC) were lower than those of pseudo second order 0.9916 (ACo), 0.9964 (HAC) and 0.9984 (ZAC). These two observations showed that the experimental data did not fit the equation of intraparticle diffusion model q_t versus $t^{(1/2)}$ or that of liquid film diffusion model $-\ln(1 - q_t/q_e)$ versus t . Large intercepts obtained by using intraparticle diffusion model suggested that the process was largely surface phenomenon and not intraparticle diffusion process. The small intercepts of plots $-\ln(1 - q_t/q_e)$ versus t , could be considered as indicating that liquid film diffusion model might have some role to play in the kinetics of adsorption of Al (III) ions onto activated carbon, ACo, HAC and ZAC.

The different models test of adsorption mechanism had presented that mechanism issued of pseudo second order model had given the best fit of experimental data and consequently, the adsorption of Al (III) ion onto activated carbons could be considered following a mechanism related to the pseudo second order kinetic model.

3.4. Thermodynamics

The adsorption equilibrium constant K_d calculated as:

$$K_d = \frac{q_e}{C_e} \quad [9]$$

Is linked to the free energy change ΔG° by the relation:

$$\Delta G^\circ = -RT \ln K_d \quad [10]$$

Plotting q_e/C_e versus q_t results of straight-line in which q_e/C_e is extrapolated when q_t leads to zero (not presented).

The enthalpy change ΔH° and entropy change ΔS° are calculated from the slope and intercept of linear plots $\ln(K_d)$ versus $1/T$ (K) given by the integrated form of Van't Hoff equation (Neetu and Chandrajit, 2015):

$$\ln K_d = \frac{\Delta S^\circ}{R} - \frac{\Delta H^\circ}{RT} \quad [11]$$

Values of energy free energy change are also obtained from the expression (12):

$$\Delta G^\circ = \Delta H^\circ - T \Delta S^\circ \quad [12]$$

The respective values of thermodynamic parameters for adsorption of Al (III) onto ACo, HAC and ZAC are given in the Table 8.

The results given in Table 8 showed that the enthalpy change values, ΔH° , for activated carbon ACo (-18.525 kJ/mol), HAC (-22.84 kJ/mol) and ZAC (-21.314 kJ/mol) are negatives indicating that the nature of adsorption process is exothermic. The negative value of entropy change, ΔS° , values for activated carbon ACo (-99.77 J.mol⁻¹.K⁻¹), HAC (-105.529 J.mol⁻¹.K⁻¹) and ZAC (-112.23 J.mol⁻¹.K⁻¹) indicated the reduced randomness at the solid/solution edge throughout the adsorption process.

The positive values of ΔG° indicated that the adsorption of Al (III) ions on the activated carbons surfaces is not a spontaneous process, but it might be realized by supplementary energy furnished by the stirring.

Conclusion

In the present study, coula edulis nut shell were successfully used as a starting material for the preparation of effective activated carbons. These activated carbons showed good adsorption capacity for removing aluminium ions from aqueous solutions.

The parameters used include: pH, initial Al (III) concentration in solutions, time and temperature.

The adsorption of Al (III) ions increased with an increase in the pH, initial concentration of Al (III) ions solution and time. The experimental data were fitted better by the Langmuir than Freundlich isotherm models.

The adsorption kinetics data followed the pseudo second order kinetic.

Thermodynamically this adsorption on activated carbons was not realised in a spontaneous manner under experimental conditions used. The adsorption was found to be exothermic during the interaction between Al (III) ions.

The results obtained indicated that the activated carbons prepared from coula edulis nut shells used as adsorbents during this study showed high adsorption capacities, which are important in adsorption technology and could be exploited in the removing of metal ions from the aqueous solutions.

References

- Amjad, M. and D.W. Knight, (2004).** A simple, two-step synthesis of 3-iodoindoles. *Tetrahedron Lett.* 45: 539-541.
- Boyd, G. E.; Adamson, A.W.; Mye, R. S. Jr, (1947).** The exchange adsorptions of ions from aqueous solutions on organic zeolites: *Journal of American Society*, G9 2836-2842.
- Denizli A., Say R. and Pikin E. (2003).** Removal of aluminum by Alizarin Yellow attached magnetic poly (2-hydroxyethyl methacrylate) beads. *React. Funct. Polym.* 55 (1) 99-107.
- Drissa Bamba, Bini Dongui, Albert Trokourey, Guessan Elogne Zoro Grah Patrick Athéba, Didier Robert, Jean Victor Wéber (2009).** Etudes comparées des méthodes de préparation du charbon actif, suivies d'un test de dépollution d'une eau contaminée au diuron. *Journal de la Société Ouest-Africaine de Chimie.* 028 ; 41 – 52.
- Estevinho, B. N., Ratola, N., Alves, A. and Santos, L. (2006).** Pentachlorophenol Removal from Aqueous Matrices by Sorption with Almond Shell Residues. *Journal of Hazardous Materials*, 137, 1175-1181.
- F. Eba, S. Gueu, A. Eya'A-Mvongbote, J. A. Ondo, B. K. Yao, J. Ndong Nlo, R. Kouya Biboutou, (2010).** Evaluation of the absorption capacity of the natural clay from Bikougou (Gabon) to remove Mn (II) from aqueous solution. *International Journal of Engineering Science and Technology.* Vol. 2(10), 5001-5016
- Freundlich, H. M. F. (1906).** Over the uptake in solution. *Zeitschrift fur Physikalische Chemie.* 57, 385–470
- Gupta, V.K.; Mittal, A.; Gajbe, V.; Mittal, J., (2008).** *Journal of Colloid Interface Science*, 319 103.
- Hayat El Hassouni, Driss Abdellaoui, Rachid Bengueddour (2013).** Kinetic and Isotherm Studies of Cu (II) Removal from Aqueous Solution Using Gigartina Acicularis Biomass. *Journal of Environment and Earth Science.* Vol.3, No.13,
- Ho Y. S., G. (1999).** McKay. Pseudo-second order model for sorption processes. *Process Biochemistry* 34 451–465
- I. Isil Gurten, Meryem Ozmak, Emine Yagmur, Zeki Aktas (2012).** Preparation and characterisation of activated carbon from waste tea using K_2CO_3 . *Biomass and bioenergy* 37, 73 – 81.
- Langmuir, I. (1918).** The uptake of gases on plane surfaces of glass, mica and platinum. *J. Am. Chem. Soc.* 40, 1362–1403
- M. Zue Mve, T. Makani and F. Eba (2016).** Removal of Mn (II) from Aqueous Solutions by Activated Carbons Prepared from Coula edulis Nut Shell. *Journal of Environmental Science and Technology.* 9 (2): 226-237,
- Miu, A. C.; Benga, O. J. (2006).** Alzheimer's Disease, 10, 179.
- Mohammad Ali Takassi, Parisa Ghashghae pour, Asadolah Farhadi, Toubha Hamule (2015).** Thermodynamic Study of Isothermal Adsorption of Aluminum Ion from Water Using Activated Carbon Adsorbent. *Journal of Water Resource and Hydraulic Engineering*, Vol. 4 (1), PP. 76-82
- Moupela C., Vermeulen C., Daïnou K. & Doucet J-L. (2011).** Le noisetier d'Afrique (Coula edulis Baill.). Un produit forestier non ligneux méconnu. *Biotechnol. Agron. Soc. Environ.*, 15(3): 485-495.
- Moupela Christian (2013).** Ecologie, dynamique des populations et intérêts économiques du noisetier d'Afrique (Coula edulis Baill.) au Gabon. *Thèse de doctorat.* Université de Liège – Gembloux Agro-Bio Tech, p1.

- Neetu Singh and Chandrajit Balomajumder (2015).** Study of Phenol adsorption from aqueous solution onto Aluminium-activated carbon: Kinetics, equilibrium and Thermodynamic. International Journal of New Technologies in Science and Engineering. Vol. 2, Issue. 4,
- Nkwaju Yanou Rachel, Ndi Julius Nsami, Belibi Belibi Placide, Kouotou Daouda, Abega Aimé Victoire, Tcheompi Marie Benadette and Ketcha Joseph Mbadcam (2015).** Adsorption of Manganese (II) Ions from Aqueous Solutions onto Granular Activated Carbon (GAC) and Modified Activated Carbon (MAC). International Journal of Innovative Science, Engineering & Technology, Vol. 2
- Nour T. Abdel-Ghani, Ghadir A. El-Chaghaby, Enas Mohamed Zahran (2015).** Cost Effective Adsorption of Aluminium and Iron from Synthetic and Real Wastewater by Rice Hull Activated Carbon (RHAC). American Journal of Analytical Chemistry, 2015, 6, 71-83
- Pesavento M, Alberti G And Bieuz R (1998).** Investigation of the speciation of aluminium in drinking waters by sorption on a strong anionic-exchange resin AG1X8. Anal. Chim. Acta 367 (1-3) 215-222.
- Pranay A Raut, Anup Chahande, Yogesh Moharkar (2015).** Various techniques for the removal of Chromium and lead from Waste water: Review. International Journal of Emerging Trends in Engineering and Basic Sciences. Vol 2, Issue 2, PP: 64-67
- Qing-Song Liu, Tong Zheng, Peng Wang, Liang Guo (2010).** Preparation and characterization of activated carbon from bamboo by microwave-induced phosphoric acid activation. Industrial Crops and Products 31 233–238.
- S. E. Ghazy and S. M. El-Morsy (2007).** Removal of Aluminum from Water Samples by Sorption onto Powdered Activated Carbon Prepared from Olive Stones. Carbon Letter; Vol. 8, No. 3, pp. 191-198
- S. Gueu, B. Yao, K. Adouby, G. Ado (2007).** Kinetics and thermodynamics study of lead adsorption on to activated carbons from coconut and seed hull of the palm tree. Int. J. Environ. Sci. Tech., 4 (1): 1-17.
- Thamilarasu P., P. Sivakumar and K. Karunakaran (2011).** Removal of Ni (II) from aqueous solutions by adsorption onto *Cajanus cajan* L Milsp seed shell activated carbons. Indian journal of Chemical Technology; Vol. 18: 414-420.
- Thebo, N. K., A. A. Simair, W. A. Sheikh, S. M. Mangrio, P. L. Nagni, S. G. Mangrio and H. M. Nizamani, (2014).** Determination of fatty acids and elements from coconut (*Cocos nucifera*) shell. Pak. J. Biotechnol., 11: 33-40.
- W. J. Weber, J. C. Morris (1963).** Kinetics of adsorption on carbon from solution. J Sanit Eng Div Am Soc Civ Engg 89 (SA2):31 – 40
- Wan Ngah, W.S. and Hanafiah, M.K.M. (2008).** Removal of Heavy Metal Ions from Wastewater by Chemically Modified Plant Wastes as Adsorbents: A Review. Bioresource Technology, 99, 3935-3948.
- Zhuo-Ya Zhong, Qi Yang, Xiao-Ming Li, Kun Luo, Yang Liu a,d , Guang-Ming Zeng (2012).** Preparation of peanut hull-based activated carbon by microwave-induced phosphoric acid activation and its application in Remazol Brilliant Blue R adsorption. Industrial Crops and Products, 37, 178–185.

Table 1: Boehm titration (Zue Mve et al., 2016)

	NaOH	NaHCO ₃	CH ₃ CONa		Previous reports on coconut shell or palm nut shell		Previous reports on coconut shell or palm nut shell
Activated Carbons	Lacton + Phenol (méq/g)	Carboxylic (méq/g)	Strong + weak acidities (méq/g)	Total Acidity (méq/g)	Total Acidity (méq/g)	Total Basicity (méq.g ⁻¹)	Total Basicity (méq.g ⁻¹)
AC ₀	0.26	0.06	0.38	0.7	(Gueu <i>et al.</i> , 2006)	0.02	(Atheba, 2009)
HAC	0.24	0.1	0.48	0.82		0.04	(Bamba <i>et al.</i> , 2009)
ZAC	0.18	0.08	0.48	0.74		0.08	

Where pH_{pzc} is the pH of point of zero charge and ACo, HAC and ZAC are activated carbon obtained without the impregnation, activated carbon obtained through the impregnation into acidic solution and activated carbon obtained through the impregnation into Zn²⁺ salt solution respectively.

Table 2: Point of zero charge, iodine number and surface area of coula edulis activated carbon (Zue Mve et al., 2016)

Activated carbon	pH _{pzc}	Iodine Number (mg/g)	Surface Area (m ² /g)
AC ₀	3	359.21	107.41
HAC	3	474.71	259.24
ZAC	3.5	558.49	224.86

Where ACo, HAC and ZAC are activated carbon obtained without the impregnation, activated carbon

obtained through the impregnation into acidic solution and activated carbon obtained through the impregnation into Zn²⁺ salt solution respectively.

Table 3: Composition analysis of *Coula edulis* nut shell ash (Zue Mve et al., 2016)

Parameters	Content (mg/Kg)	Previous report on coconut shell
Potassium (K)	660.46 ± 66.04	1511.77 mg/Kg (Thebo et al., 2014)
Calcium (Ca)	904.87 ± 30.74	556.3 mg/Kg (Thebo et al., 2014)
Magnesium (Mg)	1402.52 ± 140.2	2593.06 mg/Kg (Thebo et al., 2014)
Iron (Fe)	768.68 ± 40.24	997.97 mg/Kg (Thebo et al., 2014)
Manganese (Mn)	14.34 ± 1.43	8.67 mg/Kg (Thebo et al., 2014)
Sodium (Na)	633.17 ± 63.3	107.9 mg/Kg (Amjad et al., 2004)
Aluminum (Al)	403.73 ± 36.73	This work
Lead (Pb)	23.49 ± 3.37	0.3 mg/Kg (Amjad et al., 2004)

Table 4: FT-IR characteristics of coula edulis activated carbon (Zue Mve et al., 2016)

ACo	HAC	ZAC	FT-IR band (cm ⁻¹)
-C-C-	-C-C-	-C-C-	1033.3-1049
-C-O	-C-O	-C-O	1184.79-1240.03
-C=O and -C=C-	-C=O and -C=C-	-C=O and -C=C-	1594.15-1606.17
-C-O-C-			1099.46

Where ACo, HAC and ZAC are activated carbon obtained without the impregnation, activated carbon obtained through the impregnation into acidic solution and activated carbon obtained through the impregnation into Zn²⁺ salt solution respectively.

Table 5: Langmuir and Freundlich isotherm fitted parameters for the adsorption of Al (III) onto Coula edulis activated carbon (experimental conditions: contact time 80 minutes, pH (4), adsorbent 8 g/L and agitation speed 200 rpm at 25°C)

Activated Charbons	Langmuir				Freundlich			
	K _L (L/mg)*10 ⁻³	q _m (mg/g)	R _L	R ²	K _f (mg/g)	n	1/n	R ²
ACo	8.42	28.248	0.1055-0.4274	0.9951	3.802	3.331	0.3002	0.7786
HAC	4.28	21.69	0.1883-0.5949	0.9972	2.275	3.047	0.3281	0.7933
ZAC	10.77	35.97	0.0844-0.3685	0.9862	4.134	3.134	0.319	0.7039

Where q_m is the Langmuir monolayer maximum capacity, K_L is the Langmuir equilibrium constant, R_L is the Langmuir dimensionless factor, R² is the correlation coefficient, K_f is the Freundlich equilibrium constant, n is the intensity adsorption factor and ACo, HAC and ZAC are activated carbon obtained without the impregnation, activated carbon obtained through the impregnation into acidic solution and activated carbon obtained through the impregnation into Zn²⁺ salt solution respectively.

Tableau 6 : The pseudo first and pseudo second order kinetics parameters and statistical for the adsorption of Al (III) ions (experimental conditions: initial concentration at 244,5 mg/L, pH (4), adsorbent 8 g/L and agitation speed 200 rpm at 25°C)

Pseudo first order					
Adsorbent	q _e (exp) (mg/g)	q _e (cal) (mg/g)	K ₁ (1/min)	R ²	% déviation
ACo	14,558	8,4089	0,023	0,8758	42,24
HAC	14,378	5,867	0,0233	0,7308	59,19
ZAC	14,555	5,1305	0,269	0,821	64,75
Pseudo second order					
Adsorbent	q _e (exp) (mg/g)	q _e (cal) (mg/g)	K ₂ (1/min)	R ²	% déviation
ACo	14,558	16,393	3,59*10 ⁻³	0,9916	12,6
HAC	14,378	15,337	6,77*10 ⁻³	0,9964	6,67
ZAC	14,555	15,32	9,41*10 ⁻³	0,9984	5,26

Where q_e (exp) is the experimental monolayer maximum capacity, q_e (cal) is the theoretical monolayer maximum capacity, K₁ is the pseudo-first order constant, R² is the correlation coefficient, K₂ is the pseudo second order constant and ACo, HAC and ZAC are activated carbon obtained without the impregnation, activated carbon obtained through the impregnation into acidic solution and activated carbon obtained through the impregnation into Zn²⁺ salt solution respectively.

Table 7: Intraparticle by Weber and Morris model parameters

Activated carbons	Parameters and statistical					
	Intraparticle diffusion			Liquid film diffusion		
	K_{id1}	Intercepts	R^2	K_{id2}	Intercepts	R^2
ACo	0.9963	4.3686	0.8084	0.023	0.5489	0.8758
HAC	0.7626	6.7158	0.7363	0.0233	0.8962	0.7308
ZAC	0.6548	8.1219	0.6855	0.0269	1.0428	0.821

Where R^2 is the correlation coefficient and ACo, HAC and ZAC are activated carbon obtained without the impregnation, activated carbon obtained through the impregnation into acidic solution and activated carbon obtained through the impregnation into Zn^{2+} salt solution respectively.

Table 8: Thermodynamic parameters: The enthalpy change (ΔH°), entropy change (ΔS°) and the free energy change (ΔG°)

Activated carbons	ΔH (kJ/mol)	ΔS (J.mol ⁻¹ .K ⁻¹)	ΔG (kJ/mol)	T (K)	R^2
ACo	-18,525	-99,77	11,479	298	0,8806
			12,976	313	
			13,974	323	
			14,97	333	
HAC	-22,84	-105,529	8,607	298	0,9928
			10,19	313	
			11,245	323	
			12,301	333	
ZAC	-21,314	-112,23	12,1305	298	0,9587
			13,814	313	
			14,936	323	
			16,058	333	

Where T is the temperature in Kelvin, R^2 is the correlation coefficient and ACo, HAC and ZAC are activated carbon obtained without the impregnation, activated carbon obtained through the impregnation into acidic solution and activated carbon obtained through the impregnation into Zn^{2+} salt solution respectively.

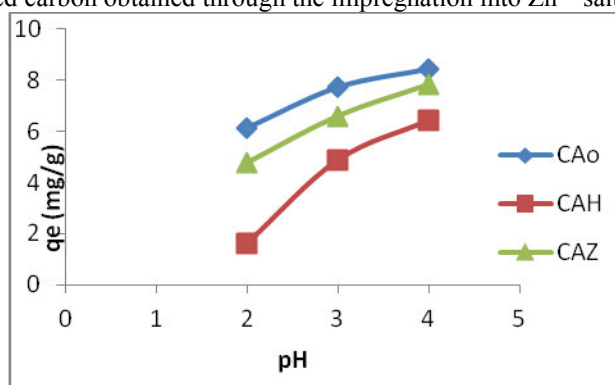


Figure 1: Variations of the amount of Al (II) ions adsorbed per unit mass as a function of pH using activated carbons: ACo, HAC and ZAC which are respectively activated carbons obtained after pyrolysis at 600°C and after pyrolysis at 600°C followed by an impregnation into acidic solution and after pyrolysis at 600°C followed by an impregnation into Zn^{2+} salt solution respectively (experimental conditions: initial concentration at 244,5 mg/L, agitation speed 200 rpm, contact time 80 minutes and adsorbent 8 g/L at 25°C).

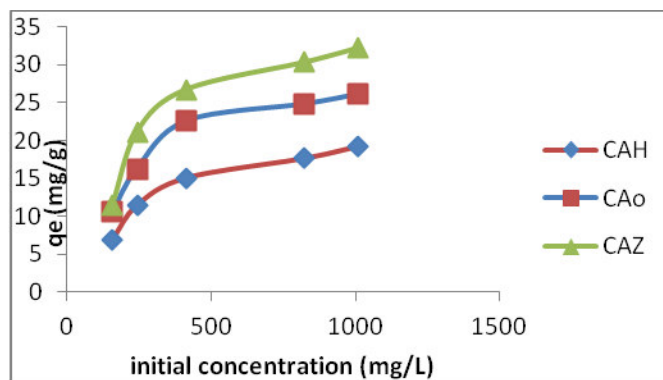


Figure 2: Variations of amount of Al (II) ions adsorbed per unit mass as a function of initial concentration of Al (II) ions solution using activated carbons: ACo, HAC and ZAC which are respectively activated carbons obtained after pyrolysis at 600°C and after pyrolysis at 600°C followed by an impregnation into acidic solution and after pyrolysis at 600°C followed by an impregnation into Zn^{2+} salt solution respectively (experimental conditions: contact time 80 minutes, pH(4), adsorbent 8 g/L and agitation speed 200 rpm at 25°C)

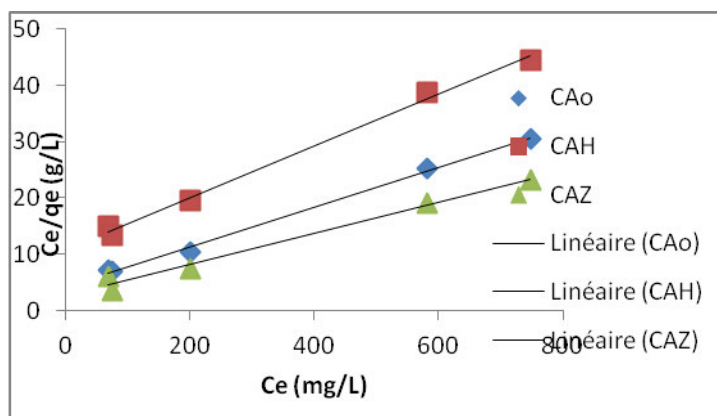


Figure 3: Plots of variations of the ratio of the equilibrium concentration on amount Al (III) adsorbed per unit mass as a function of the equilibrium concentration related to the Al (III) ions adsorption using ACo, HAC and ZAC which are respectively activated carbons obtained after pyrolysis at 600°C and after pyrolysis at 600°C followed by an impregnation into acidic solution and after pyrolysis at 600°C followed by an impregnation into Zn^{2+} salt solution respectively (experimental conditions: contact time 80 minutes, pH (4), adsorbent 8 g/L and agitation speed 200 rpm at 25°C)

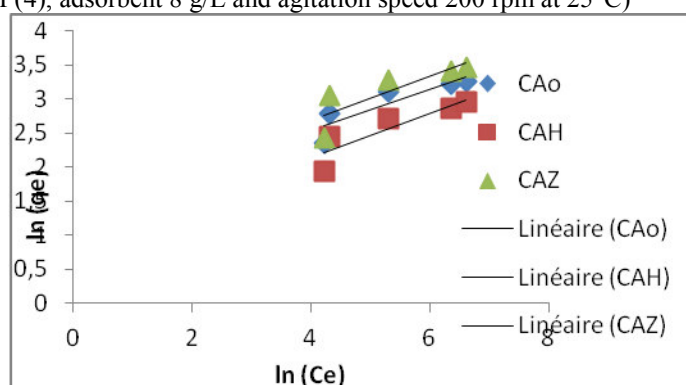


Figure 4: Plot of variations of the logarithm of amount Al (III) adsorbed per unit mass as a function of the logarithm of equilibrium concentration of Al (III) ions using ACo, HAC and ZAC which are respectively activated carbons obtained after pyrolysis at 600°C and after pyrolysis at 600°C followed by an impregnation into acidic solution and after pyrolysis at 600°C followed by an impregnation into Zn^{2+} salt solution respectively (experimental conditions: contact time 80 minutes, pH (4), adsorbent 8 g/L and agitation speed 200 rpm at 25°C)

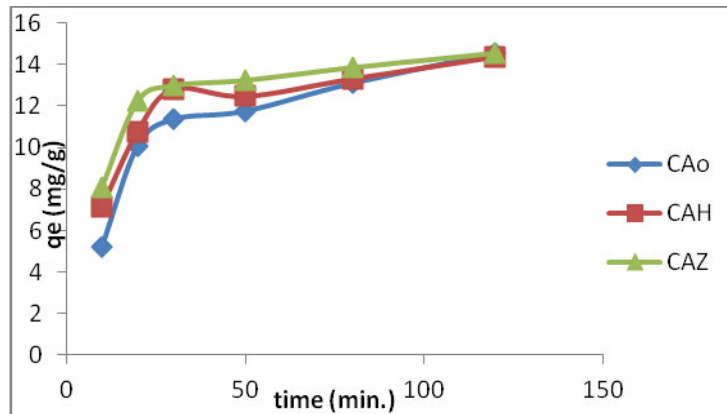


Figure 5 : Variations of amount of Al (III) ions adsorbed per unit mass as a function of contact time using ACo, HAC and ZAC which are respectively activated carbons obtained after pyrolysis at 600°C and after pyrolysis at 600°C followed by an impregnation into acidic solution and after pyrolysis at 600°C followed by an impregnation into Zn²⁺ salt solution respectively (experimental conditions: initial concentration at 244,5 mg/L pH (4), adsorbent 8 g/L and agitation speed 200 rpm at 25°C)

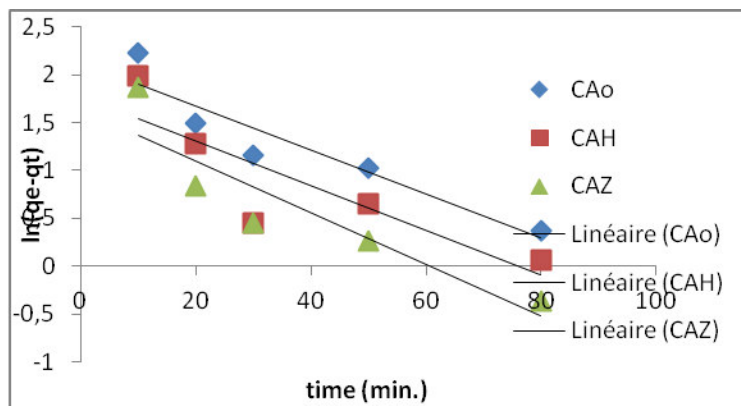


Figure 6 : plots of variations of the logarithm of difference between the equilibrium Al (III) ions uptake and Al (III) ions uptake per unit mass for any time as a function of time (Lagergren first-order kinetic model) for the adsorption of Al (III) ions using ACo, HAC and ZAC which are respectively activated carbons obtained after pyrolysis at 600°C and after pyrolysis at 600°C followed by an impregnation into acidic solution and after pyrolysis at 600°C followed by an impregnation into Zn²⁺ salt solution respectively (experimental conditions: initial concentration at 244,5 mg/L, pH (4), adsorbent 8 g/L and agitation speed 200 rpm at 25°C)

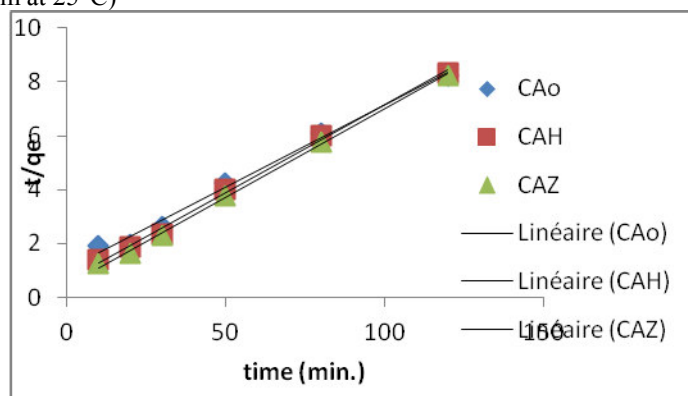


Figure 7: Plots of variations of the ratio of time on adsorption capacity related any time as a function of time (pseudo- second-order kinetic model) for the adsorption of Al (III) ions for the adsorption of Al (III) ions using ACo, HAC and ZAC which are respectively activated carbons obtained after pyrolysis at 600°C and after pyrolysis at 600°C followed by an impregnation into acidic solution and after pyrolysis at 600°C followed by an impregnation into Zn²⁺ salt solution respectively (experimental conditions: initial concentration at 244,5 mg/L, pH (4), adsorbent 8 g/L and agitation speed 200 rpm at 25°C)

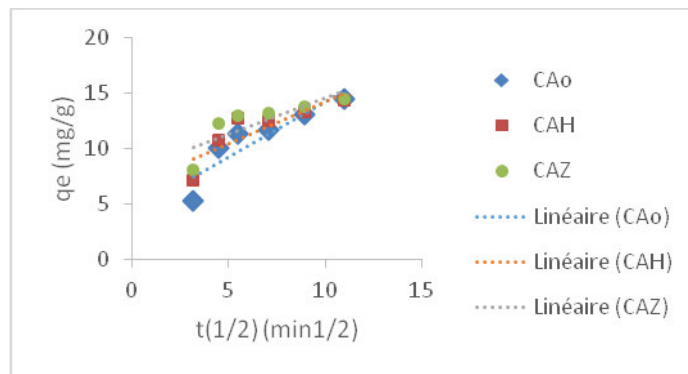


Figure 8: Intraparticle diffusion plots for Al (III) ions adsorbed on activated carbon (initial concentration: $C_0=244,5$ mg/L, pH (4), adsorbent 8 g/L and agitation speed 200 rpm at 298K and at pH4)

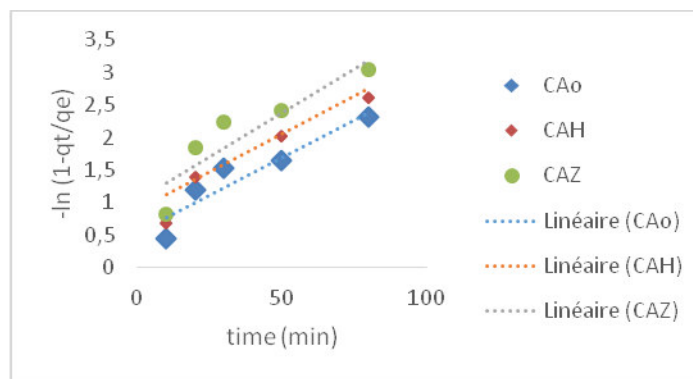


Figure 9: Liquid film diffusion plots for Al (III) ions adsorbed on activated carbon (initial concentration: $C_0=244,5$ mg/L, pH (4), adsorbent 8 g/L and agitation speed 200 rpm at 298K and at pH4)

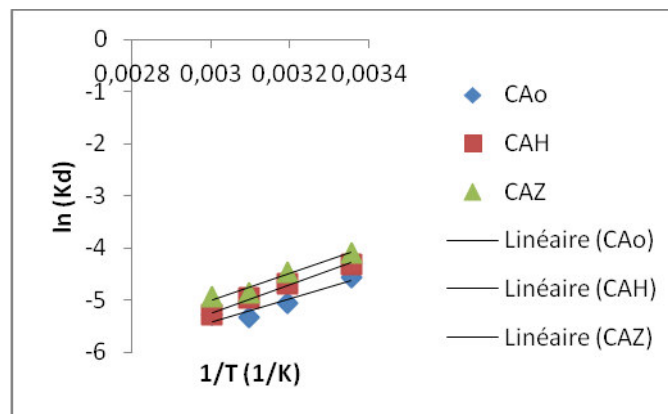


Figure 10: Plots of $\ln(K_d)$ versus $1/T$ for adsorption of Al (III) ions in aqueous solution